Toward the full control of NCPA with the pyramid wavefront sensor: mastering the optical gains

Arnaud Striffling, Cedric Taissir Heritier, Jean-François Sauvage, Alexis Carlotti, Olivier Fauvarque, Romain Fetick, Benoit Neichel, Thierry Fusco

AO4ELT7 - June 2023 - Avignon

Toward the full control of NCPA with the pyramid wavefront sensor: mastering the optical gains

A. Striffling[a,b,c], C.-T. Héritier[a,c], J.-F. Sauvage[a,c], A. Carlotti[b], O. Fauvarque[d], R.J.-L. Fétick[a,c], B. Neichel[c], and T. Fusco[a,c]

[a]DOTA, ONERA, F-13661 Salon cedex Air - France
[b]Univ. Grenoble Alpes, CNRS, IPAG, 38000 Grenoble, France
[c]Aix Marseille Univ, CNRS, CNES, LAM, Marseille, France
[d]Ifremer, RDT Research and Technological Development, F-29280 Plouzané, France

ABSTRACT

The pyramid wavefront sensor is an asset for an AO system thanks to its sensitivity. However, because its a nonlinear sensor it comes with operational challenges. A convolutional method and a gain sensing camera allow to track the optical gains, which encode the sensitivity variations due to the nonlinearities. Tracking and compensating the optical gains is necessary to perform extreme adaptive optics and to operate the pyramid off-zero to compensate for the NCPA.This study focuses on the reliability of this method. A numerical twin of the bench PAPYRUS, developed for this study, shows a improvement of the performance by a factor 2.7 on the Strehl Ratio when compensating for the optical gains. The convolutional method is implemented for the PAPYRUS bench, allowing the first on-sky tracking of optical gains. The next main steps are to compensate for the optical gains in real-time, then to offset the pyramid in order to optimise fiber-injection, to compensate for NCPA and to provide AO generated dark hole for high-contrast imaging.

Keywords: High contrast imaging, pyramid, NCPA, adaptive optics, wavefront sensing

Further author information:
A. Striffling, E-mail: arnaud.striffling@onera.fr

1. INTRODUCTION

In 1995 the first exoplanet was discovered at Observatoire de Haute Provence (OHP) [14] around a solar type star. 30 years later, more than 5000 exoplanets have been detected, mainly using indirect methods. The next step aims at using direct imaging techniques to characterize the chemical content of their atmosphere and better understand their formation process.

Toward this goal, one major instrumental challenge must be overcome: the very faint light coming from the planet must be separated from the one of its very bright neighbouring star. The typical angular separation between the star and the planet is indeed only of a fraction of arcsecond for nearby stars, and the flux ratio reaches 10^6 (jupiter planets) to 10^9 (rocky planets). The recipe to reach such an ambitious objective consists of combining an extremely large telescope to provide the angular resolution, an eXtreme performance Adaptive Optics (XAO) to correct for the atmospheric turbulence and a high-contrast instrument equipped with high resolution spectroscopic capabilities [2] to mask the starlight, reveal the planet photons and derive a spectra of the planet atmosphere.

All the first light SCAO instruments [6, 1, 17] of the ELT [18] will be equipped with a Pyramid WFS (PyWFS) [15] to benefit from a compact design for the WFS detector, versatility with the use of Tip/Tilt modulation and higher sensitivity with respect to the Shack-Hartmann WFS [19]. However, the PyWFS exhibits nonlinearities that must be properly compensated, in particular in the context of high contrast instruments that require a perfect correction of both dynamic and static aberrations. In this paper, we focus on the use of the PyWFS with the goal to master its nonlinearities to optimize the coupling with a high contrast instrument.

In particular, we will focus on the optical gain estimation. The optical gains are a quantifier of the PyWFS nonlinear behaviour. To measure them we use the convolutional formalism [9] coupled to a focal plane camera [3]. This method is now implemented on PAPYRUS AO bench at OHP, to experience it on sky.

2. AO LOOP WORKING WITH CONTROLLED ABERRATIONS

The goal of AO is to correct all the aberrations from those induced by the atmosphere to the static ones inherent to the bench, like the non common path aberrations. However, in some particular cases it is interesting to introduce some controlled aberrations to perform injection in an optical fiber, or dark hole techniques [13] for high-contrast enhancement for example.

2.1 The Non Common Path Aberrations

An adaptive optics system (AO) is classically composed of a deformable mirror (DM), a real-time computer (RTC) and a wavefront sensor (WFS). The system is usually operated in a feedback loop where the WFS converts phase residuals into measurable signals related to the aberrated wavefront. These signals are converted by the RTC into commands to be applied on the DM and compensate the optical aberration sensed by the WFS.

Thus, the AO system is placed upstream of the imaging camera and extracts a fraction of the light which is sent to the WFS thanks to a dichroic beamsplitter (DBS). The optical paths of the sensing arm, δ_{WFS} on figure 1, and of the imaging arm, δ_{Ima}, are different due to their various optical components. Because it is impossible to reach a perfect alignment, an optical path difference appears, the wavefronts are not identical at the end of each arm: the system is facing non-common path aberration (NCPA). For instance, in the case of SPHERE, the best alignment led to 50 nm of static aberrations [16].

If the AO loop is closed without compensation of the NCPA, the wavefront will be flatten from the WFS perspective. The differential aberration ($\delta_{\mathrm{Ima}} - \delta_{\mathrm{WFS}}$) is sent on the imaging arm, which leads to the deterioration of the point spread function (PSF) on the astronomical instrument. To get a flatten wavefront on the imager we can set the opposite of the differential aberration as an offset to the wavefront sensor that consequently works around a non-zero regime. This operation comes with a cost, the pyramid WFS being nonlinear, it reduces even more its dynamic range and lower its sensitivity.

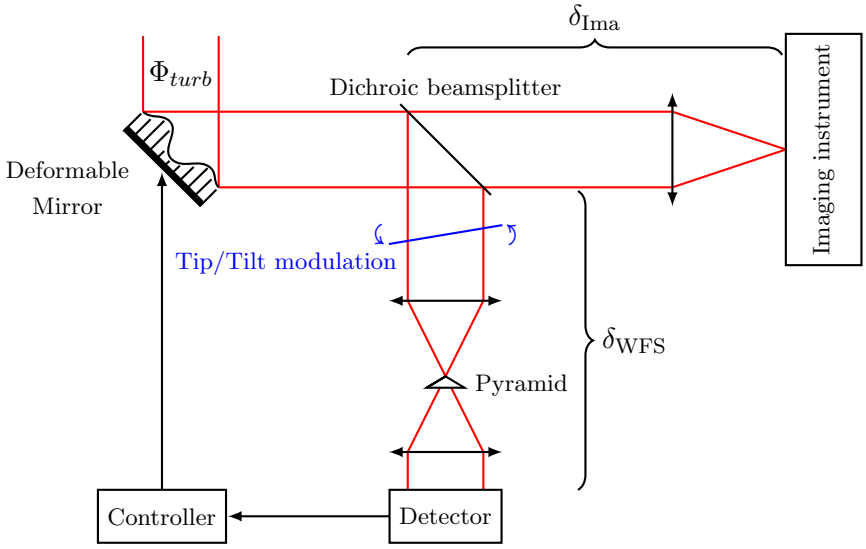

Figure 1. Simple schematic of an AO loop using a Pyramid wavefront sensor.

2.2 Dealing with PyWFS offset signals for high contrast applications

As mentioned in the introduction, we also want to combine the XAO system with a high contrast arm and high contrast fiber-spectograph. Accurate injection of the planet's light into the fiber requires an absolute positionning of the PSF on the tip of the monomode fiber at a fraction of λ/D accuracy, which requires a perfect control of the tip/tilt with respect to the AO guide star. Moreover, in order to enhance the performance of a coronagraphic system, it can be necessary to use dark hole techniques to locally increase the contrast in the PSF. These later requires to intentionally add phase aberrations, called dark hole maps, on the imaging path upstream of the coronagraph.

Those two aberrations, the tip/tilt and the dark hole maps, can be integrated in the AO in the same way as the NCPA are compensated, by changing the offset signal of the WFS. In this case we don't want to correct for aberrations, but to introduce on purpose aberrations that are perfectly controlled. From now on all those aberrations will be referred as NCPA.

2.2.1 Absolute Tip/Tilt for fiber injection

Injecting light into a single-mode fiber (SMF) at the output of an AO system requires a high-precision centering. The stability required for a good injection is below 0.1 λ/D [7]. The loop is closed on the reference star and the exoplanet drifts around it, in the focal plane, because of the rotation of the field of view during the observation period. A fine tuning of the tip-tilt is required to compensate for the drift by shifting the AO-corrected PSF at the entrance of the SMF.

2.2.2 Dark-hole phase maps for high-contrast imaging

One way to create a dark hole, which is a localized increase of the contrast in the PSF after a coronagraph, is to use aberrated phase maps. They are specifics to each observation and coronagraphic system. These aberrations modify the light distribution of the PSF in order to relocate photons of the star from the location of the exoplanet to elsewhere in the focal plane, *cf* figure 2. The benefit of creating dark hole with phase mask rather than amplitude mask is twofold. Firstly, no photons are removed and secondly, it is possible to update the mask when the AO system is operating.

2.3 Dealing with static and quasi-static aberrations

Whether it is compensating NCPA (middle-order frequencies), mastering an absolute tip/tilt or creating dark hole map (high-order frequencies), the operation is the same: offsetting the wavefront sensor signals [8]. This technique allows on-the-fly modifications of those aberrations.

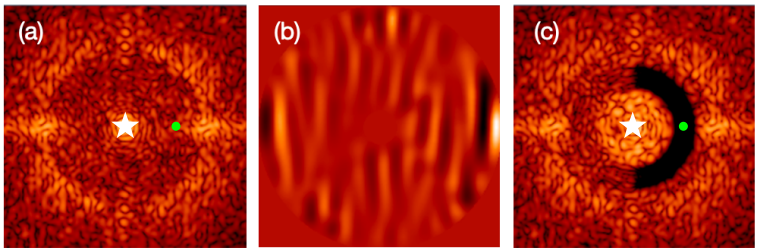

Figure 2. Illustration of a phase dark hole technique, the green dot represents the exoplanet; (a) PSF with a coronagraph only; (b) phase dark hole map; (c) impact of the applied dark hole map on the coronagraphic PSF.

However, the nonlinear behaviour of the PyWFS requires to adjust the amplitude of the offset signal, because the sensitivity depends on the amount of aberration to measure. From there, it is imperative to quantify those nonlinearities, otherwise the applied offset signal is incorrect.

3. THE PYRAMID: A NON LINEAR WAVEFRONT SENSOR

3.1 Describing the nonlinearities: the optical gains

The PyWFS is a nonlinear sensor, which converts a variation of phase into a variation of pixel intensity on a detector. Using the formalism introduced in [9], the output signal for a given phase Ψ can be written:

$$I(\Psi) = I_{\text{constant}} + I_{\text{linear}}(\Psi) + I_{\text{quadratic}}(\Psi) + ... \tag{1}$$

with I_{constant} independent of the input phase, which is therefore subtracted from the total intensity, giving the differential intensity:

$$\Delta I(\Psi) = I_{\text{linear}}(\Psi) + I_{\text{quadratic}}(\Psi) + ... \tag{2}$$

The sensor can be considered as locally linear with a sensitivity specific to each mode ϕ_i, $\Delta I(a\phi_i) = I_{\text{linear}}(a\phi_i)$, with an amplitude a small enough to avoid eventual saturation and non-linear effects. During the calibration process the differential intensity of each mode of a basis is recorded, following a push-pull method. The linear approximation is represented using the dashed black curve of the figure 3(a). This curve is tangent to the real behaviour (blue curve) of the PyWFS around the calibration point. During on-sky operations the incoming phase affects the energy distribution in the focal plane at each frame and is different from the one used for the calibration. This affects the sensitivity (red curve) and since the pyramid is not equally sensitive to all spatial frequencies, each mode is affected differently. Under the diagonal approximation (no modal confusion [5]), this mis-match between calibration and operating regime is encoded in a quantity called the optical gains (OG), represented as the green arrow on figure 3(a). The OG can be computed as [4]:

$$g = \frac{\text{diag}\left({}^{\text{t}}\text{D}_{\text{sky}}.\text{D}_{\text{calib}}\right)}{\text{diag}\left({}^{\text{t}}\text{D}_{\text{calib}}.\text{D}_{\text{calib}}\right)} \tag{3}$$

g is a vector containing the optical gains of all modes, D_{calib} the calibration interaction matrix and D_{sky} a interaction matrix measured around an aberrated phase to measure.

3.2 Working off-zero: the importance of compensating optical gains

Compensating for the optical gains, with the PyWFS used around zero, improves the performance of the AO loop. As shown on the figure 3(a) the loss of sensitivity during the on-sky regime leads to an under-estimation of the modes measured in the incoming phase. A similar issue appears when working off-zero, the sensitivity of the sensor is reduced, *cf* figure 3(b). Compensating the optical gains in the AO loop allows to regain performance. Because OG are a reduction of the sensitivity, the reconstructor needs to be upscaled by the inverse of the estimated OG, as shown on figure 4 in the OG compensation part.

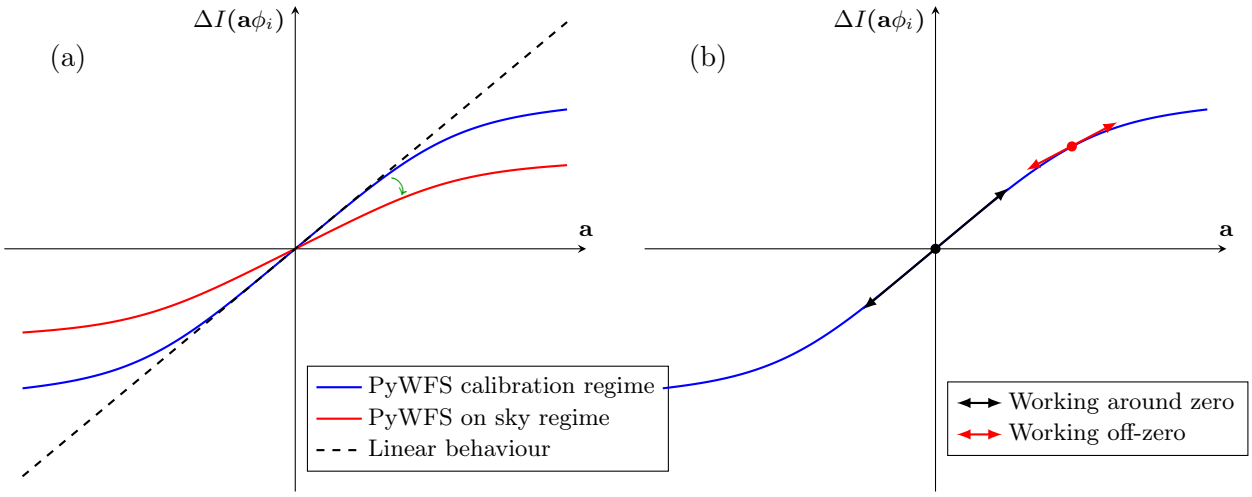

Figure 3. Differential intensity as the output signal of the pyramid for a given mode ϕ_i depending on the amplitude a of the mode ; (a) impact of the optical gains on the pyramid signal ; (b) effect of working off-zero.

A second effect of the nonlinearities arises when dealing with NCPA. The nonlinearities will create a dependency of the signal offset with respect to the aberrations level. In other term, the WFS signal offset required to compensate for an specific quantity of NCPA varies with seeing value. In the best case, the NCPA effectively introduced are smaller than wanted. In the worst case, they are larger than wanted and might drive the WFS to saturation and the loop to divergence. This is called the NCPA catastrophe [4]. The solution for dealing with this problem is to be able to monitor the optical gains with respect to seeing, and to scale the WFS signal offset accordingly. This is presented in the NCPA scaling part of the figure 4.

It is therefore essential to have an optical gain estimator, which compute an estimate (in blue, fig 4) of the true OG (in red, fig 4). Such an estimator, enabling real-time OG tracking, is made possible using a mathematical based formalism and a focal plane camera.

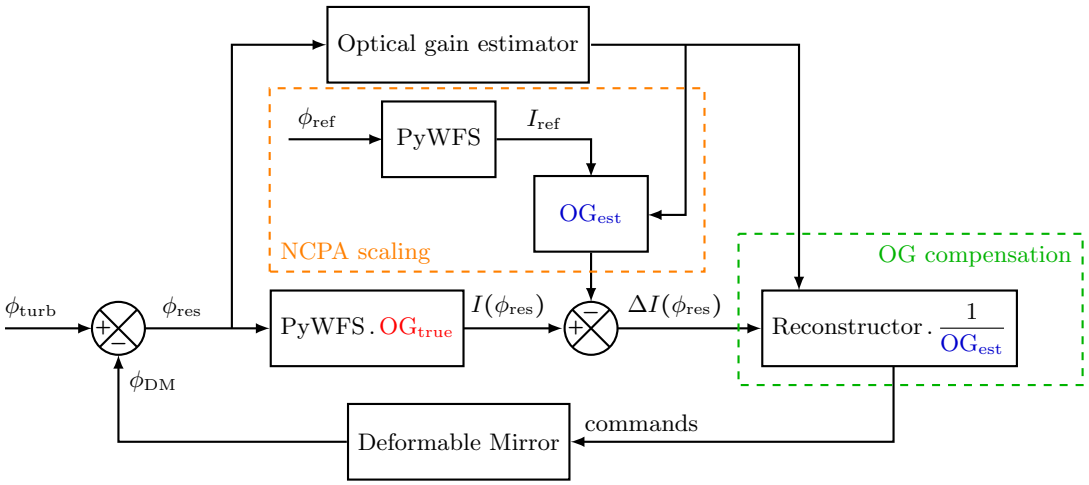

Figure 4. Block diagram of the AO loop representing the action of the optical gains to avoid the NCPA catastrophe and to regain performance.

4. THE CONVOLUTIONAL MODEL: A FAST AND ACCURATE WAY TO COMPUTE OPTICAL GAINS

As mentioned in equation (3), the use of two interactions matrices gives an accurate estimation of optical gains. This method can easily be used during numerical simulations although it requires a lot of computation

time. However, the on-sky interaction matrix would require to calibrate the system for each frame, which is not accessible at all.

Another method, based on a convolutional model [9] enables real-time estimation of optical gains. The idea behind this model is to measure the impulse response (IR) of the sensor to a phase Dirac distribution (a null phase map with a single nonzero point in the pupil). The impulse response fully characterises the system in only one optical propagation. The IR is convoluted with a modal basis to get an interaction matrix with a fast computation.

The IR can be determined with an analytical formula [3]:

$$\mathrm{IR} = 2\Im\left[\bar{\hat{m}}\left(\widehat{m \times \Omega_\phi}\right)\right] \tag{4}$$

with $\Im[\cdot]$ representing the imaginary part, m the pyramid phase mask and Ω_ϕ the modulated PSF. To get such an image of the modulated PSF in practice, a beamsplitter is placed just upstream the pyramid, and a camera, called the Gain Sensing Camera (GSC), is placed in the corresponding lateral focal plane, *cf* figure 5. The modulated PSF is the witness of several quantities that are needed to compute optical gains: the tip/tilt modulation path, the telescope's pupil, and the phase aberrations.

The analytical formula to get the optical gains is the following:

$$g_i = \frac{\int \widehat{\mathrm{IR}_\phi}\ \widetilde{\mathrm{IR}_\mathrm{c}}\ \hat{\phi}_i\ \check{\phi}_i}{\int \widehat{\mathrm{IR}_\mathrm{c}}\ \widetilde{\mathrm{IR}_\mathrm{c}}\ \hat{\phi}_i\ \check{\phi}_i} \qquad \forall\ i \in [\![1, n_\mathrm{modes}]\!] \tag{5}$$

where IR_ϕ is the impulse response computed around the aberrated wavefront, IR_c is the impulse response in calibration and ϕ_i the i-th mode of the modal basis. The blue elements of (5) are only computed once during the initialization of the AO system. Then, during the observation, the GSC acquires images of the modulated aberrated PSF to compute IR_ϕ on the fly with (4), leaving only n_modes Fourier transforms, multiplications, sums and divisions. Ideally we would like the GSC to track the OG for every frame of the pyramid WFS: at every frame, the aberrations have evolved, and so do the OG.

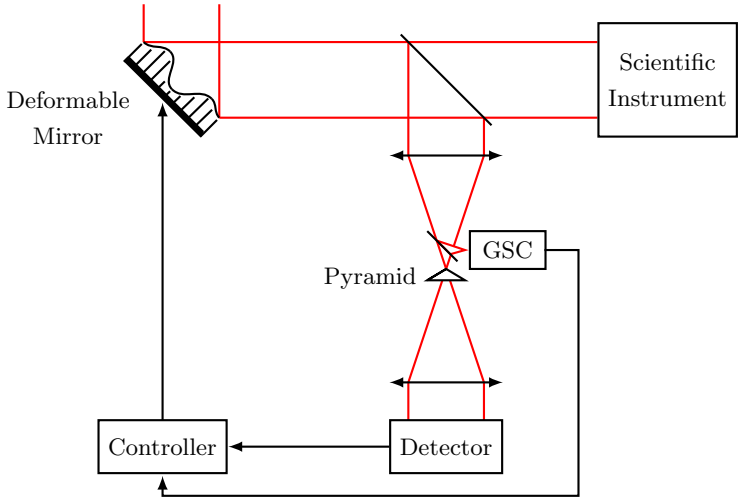

Figure 5. Gain sensing camera positioning in the AO bench.

The figure 6 shows a comparison between an end-to-end simulation of an AO loop using OOPAO [12] and the convolutional model for the computation of the optical gains for a given phase screen. The simulation parameters are presented on the table 1. The graphs show the OG for each of the KL modes controlled by the AO system, estimated with E2E simulation, equation (3), and estimated by the convolutional model, equation (5), both in the diagonal approximation. On the left the OG are computed for an uncorrected turbulence and for a AO-corrected

Atmosphere	5 layers following Von-Karman PSD
Resolution	80 pixels in the telescope diameter
Telescope	$D = 8$ m – no central obstruction
Deformable mirror	20x20 actuators
Control basis	Karhunen-Loève: 300 modes
r_0	20 cm @ 650 nm

Table 1. Simulation parameters of a VLT-like system.

turbulence on the right. Both methods give similar values of OG with an identical profile. The inflection point is directly linked to the modulation radius. The convolutional model being based on the approximation of a infinite pupil, it is less precise and the curve appears smoother. However, it is the general trend of the curve which is important to get, more than the tiny variations between modes, that have less impact. The estimation of optical gains using the convolutional approach is therefore good enough for modelizing the nonlinearities of the PyWFS.

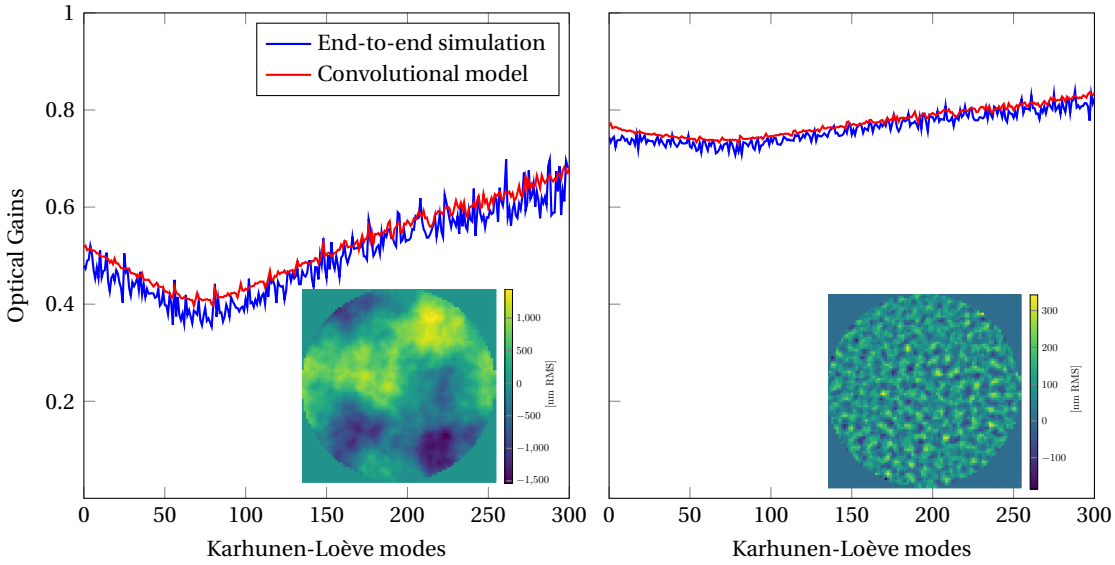

Figure 6. Computation of opticals gains on the same phase screen using both end-to-end simulation and convolutional model. On the left with uncorrected turbulence, on the right with AO-corrected turbulence.

5. PAPYRUS AO BENCH: PERFORMANCE AND OG ESTIMATION

This last part presents simulation results of compensating for optical gains to regain performance and experimental optical gains estimation, with the PAPYRUS AO bench [11]. This bench is installed on the T152 telescope of OHP. The main features of the system are the following:

- 17-by-17 actuators deformable mirror from ALPAO;
- pyramid wavefront sensor working in the broadband visible, with the WFS camera being the OCAM2K electron multiplying CCD from First Light Imaging;
- RTC running at 500 Hz on Matlab.

A numerical twin of the bench developed on OOPAO is used for the simulation, with the parameters shown of table 2.

Atmosphere	5 layers following Von-Karman PSD
Resolution	160 pixels in the telescope diameter
Telescope	D = 1.52 m – T152 real pupil
Deformable mirror	17x17 actuators
Control basis	Karhunen-Loève: 140 modes
Sensing	658 nm (R-band)
Loop frequency	500 Hz
PyWFS Modulation	5 λ/D

Table 2. Simulation parameters of the PAPYRUS numerical twin.

5.1 Compensating the OG in simulation to improve performance

The simulation presented on the figure 7 shows the evolution of the Strehl ratio (under the Maréchal approximation) in the visible for different r_0. The loop is running with a 0,5 integator gain and two frames delay. At OHP the statistics of r_0 range from 4 cm for the worst nights to 8 cm for the best ones. The blue curve with red dots illustrate the current simulated performance of the system on-sky. The dashed blue curve is the fundamental limit due to fitting error driven by the number of actuators in the diameter and the pitch of the DM.

The blue curves with green squares and blue triangles show the performance that we could reach when compensating for the OG frame-by-frame or every 3 frames with the GSC and the convolutional model. The red curve illustrate the gain in SR between the performance without OG compensation and frame-by-frame OG compensation. For r_0 values under 4 cm the loop diverges. What is interesting is that the gain of performance is much important for low r_0 than for higher r_0. This is linked to the fact that the stronger the turbulence is, the lower are the optical gains. In that case their compensation leads to higher increase of performance.

The slight improvement of the performance while compensating OG every frame rather than every 3 frames shows how fast they evolve. Then, it is slightly preferable to compensate them frame-by-frame rather than on time average, which is exactly the aim of our system.

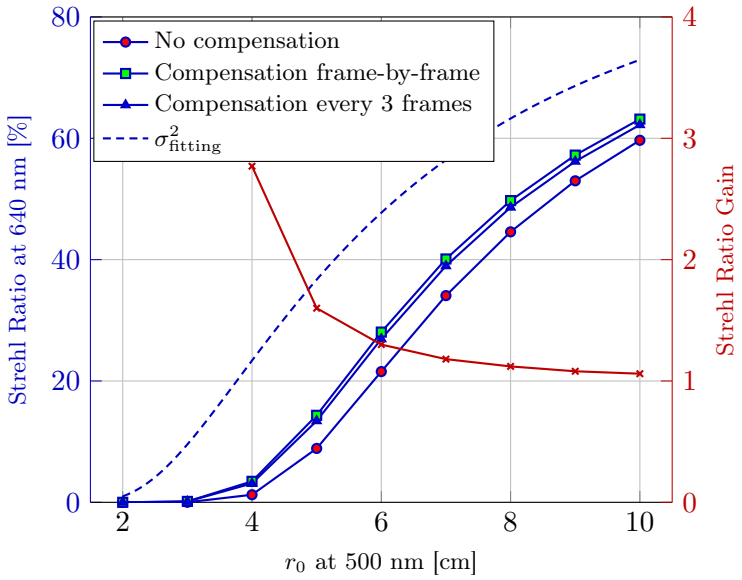

Figure 7. Simulated performance if optical gains where compensating frame-by-frame or every 3 frames.

5.2 Computation of OG on-sky with PAPYRUS

We implemented the convolutional approach for estimating the OG on experimental data from the Papyrus AO bench. We performed a campaign of observation of three nights in May 2023 dedicated to GSC integration in the Papyrus RTC and on-sky tests. Our goal is to see if we can accurately estimate the optical gains with the convolutional model. For that we did 3 experiments with a dataset. While closing the loop on Arcturus with Papyrus we recorded long-exposure PSF, the commands sent to the DM, and the GSC's frames. From these data, we were able to estimate the OG with three different methods, and cross-checked them:

(1) With the on-sky frames coming from the GSC we are able to estimate the optical gains, in blue, so with experimental data.

(2) With the long exposure on-sky PSF and a fitting algorithm [10] we were able to estimate the average seeing, allowing us to simulate an atmosphere with the right r_0 on OOPAO and estimate the optical gains using the convolutional approach on simulated data, in green on figure 8.

(3) Lastly, the commands sent to the DM in closed-loop we were able to recreate at best the low orders of the atmosphere even if biased by OG and combine them with a simulation of the high orders on OOPAO and estimate the optical gains in simulation, in red.

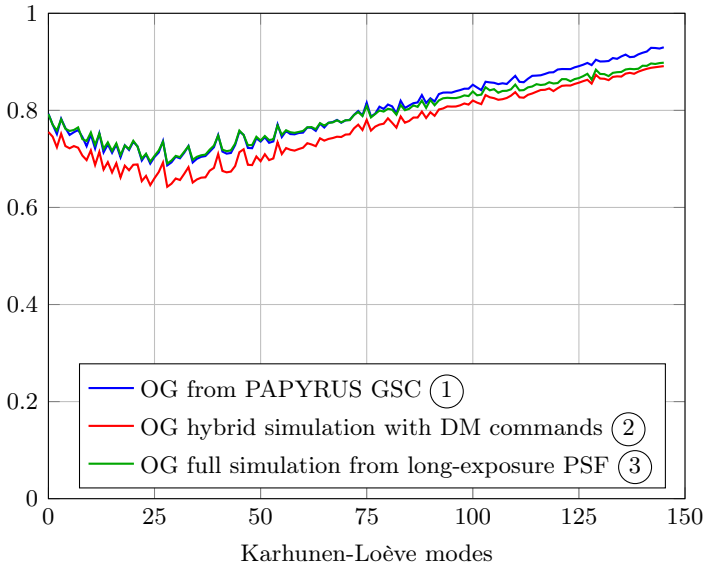

Figure 8. Comparison of time average optical gains computed following 3 different procedures: on experimental data, with hybrid experimental-simulated data, with fully simulated data.

On the method (1) the optical gains are estimated with the highest accuracy with regard to experimental conditions. They take into account all the aberrations seen by the wavefront sensor, the real wind speed and the real seeing as well as all the telescope effects. They act as our reference since we are confident that the OG estimated from the GSC are consistent with the value expected (see figure 6).

The method (2) is hybrid to (i) capture the temporal evolution of the low order modes by replaying the DM commands at the loop frame-rate and (ii) simulate high order residuals using OOPAO phase screens computed with an estimation of r_0 obtained from a long exposure PSF fitting. In this situation, we notice that the estimated OG have the same shape as our reference (blue curve) but with a constant offset. Understanding the origin of this offset is currently under investigation (estimation of r_0?, scaling of the experimental DM commands to adapt them to the simulation tool?).

The method (3) is based on phase screens computed entirely in OOPAO using the r_0 extracted from the PSF fitting and the wind speed is adjusted to fit the experimental OG (blue curve). In this case, the telescope effects (dome seeing) are not included, which could explain the difference in shape between the green and blue curve.

These preliminary results provide already a consistent estimation of the OG, with small differences, giving confidence in the method, model and analysis developed. Further investigation on the effect of each parameter (r_0, wind-speed and telescope effects) on the optical gains is required to finely tune and characterise the estimation of these parameters.

6. CONCLUSION

To address the problematic of pyramid optical gains variation associated to NCPA compensation, we consider the method developed in [3] to perform a fast online optical estimation. The goal is to validate experimentally the method using the PAPYRUS platform.

In this study, we first recalled the formalism and method to estimate the optical gains from a focal plane camera. We applied it in simulation using a numerical twin of PAPYRUS to study the associated performance. We demonstrated that a gain of performance up to a factor 2.7 in Strehl-Ratio is expected for low values of r_0.

As a first experimental result, we were able to obtain the first on-sky measurements optical gains using a GSC during a measurement campaign at OHP. In this case, no compensation is applied and only a monitoring of the optical gains was implemented. We challenged these first estimations with numerical simulations that showed very good consistency, giving good confidence in the feasibility of the method and in the accuracy of our numerical twin.

This first milestone paves the road to a full demonstration of the method where the optical gains are estimated using the GSC frames and fed to the reconstructor at a high frame-rate. This work is currently being implemented in the PAPYRUS RTC to provide a full experimental validation of the method.

The next step will be to address the problematic of operating the pyramid off-zero, NCPA and controlled offsets, to prepare the arrival of high-contrast, imaging and spectroscopic instruments [2].

ACKNOWLEDGMENTS

This work benefited from the support of the the French National Research Agency (ANR) with WOLF (ANR-18-CE31-0018), APPLY (ANR-19-CE31-0011) and LabEx FOCUS (ANR-11-LABX-0013); the Programme Investissement Avenir F-CELT (ANR-21-ESRE-0008), the Action Spécifique Haute Résolution Angulaire (ASHRA) of CNRS/INSU co-funded by CNES, the ECOS-CONYCIT France-Chile cooperation (C20E02), the ORP-H2020 Framework Programme of the European Commission's (Grant number 101004719), STIC AmSud (21-STIC-09), the Région Sud and the french government under the France 2030 investment plan, as part of the Initiative d'Excellence d'Aix-Marseille Université - A*MIDEX, program number AMX-22-RE-AB-151.

References

[1] Thomas Bertram et al. "Single conjugate adaptive optics for METIS". In: *Adaptive optics systems vi*. Vol. 10703. SPIE. 2018, pp. 357–367.

[2] Alexis Carlotti et al. "On-sky demonstration at Palomar Observatory of the near-IR, high-resolution VIPA spectrometer". In: *Ground-based and Airborne Instrumentation for Astronomy IX*. Aug. 2022. DOI: 10.1117/12.2628937.

[3] Vincent Chambouleyron et al. "Focal-plane-assisted pyramid wavefront sensor: Enabling frame-by-frame optical gain tracking". In: *Astronomy & Astrophysics* 649 (May 2021). DOI: 10.1051/0004-6361/202140354.

[4] Vincent Chambouleyron et al. "Pyramid wavefront sensor optical gains compensation using a convolutional model". In: *Astronomy & Astrophysics* 644 (Dec. 2020). DOI: 10.1051/0004-6361/202037836.

[5] Mahawa Cisse et al. "The phase-shifted Zernike wave-front sensor". In: *Adaptive Optics Systems VIII*. Montréal, Canada: SPIE, Aug. 2022. DOI: 10.1117/12.2628885.

[6] Yann Clénet et al. “The MICADO first-light imager for the ELT: towards the preliminary design review of the MICADO-MAORY SCAO”. In: *Adaptive Optics Systems VI*. Vol. 10703. SPIE. 2018, pp. 346–356.

[7] M. El Morsy et al. “Validation of strategies for coupling exoplanet PSFs into single-mode fibres for high-dispersion coronagraphy”. In: *Astronomy & Astrophysics* 667 (Nov. 2022). DOI: 10.1051/0004-6361/202243408.

[8] S Esposito et al. “On-sky correction of non-common path aberration with the pyramid wavefront sensor”. In: *Astronomy & Astrophysics* 636 (2020), A88.

[9] Olivier Fauvarque et al. “Kernel formalism applied to Fourier-based wave-front sensing in presence of residual phases”. In: *Journal of the Optical Society of America A* 36.7 (July 2019). DOI: 10.1364/JOSAA.36.001241.

[10] R. J. L. Fétick et al. “Physics-based model of the adaptive-optics-corrected point spread function: Applications to the SPHERE/ZIMPOL and MUSE instruments”. In: *Astronomy & Astrophysics* 628 (Aug. 2019). DOI: 10.1051/0004-6361/201935830.

[11] Romain JL. Fétick et al. “PAPYRUS: one year of on-sky operations”. In: *AO4ELT-7 proceedings* (2023).

[12] Cédric Taïssir Héritier et al. “Object oriented python adaptive optics (OOPAO)”. In: *AO4ELT-7 proceedings* (2023), https://github.com/cheritier/OOPAO.

[13] F Malbet, JW Yu, and M Shao. “High-dynamic-range imaging using a deformable mirror for space coronography”. In: *Publications of the Astronomical Society of the Pacific* 107.710 (1995), p. 386.

[14] Michel Mayor and Didier Queloz. “A Jupiter-mass companion to a solar-type star”. In: *Nature* 378.6555 (Nov. 1995). DOI: 10.1038/378355a0.

[15] Roberto Ragazzoni. “Pupil plane wavefront sensing with an oscillating prism”. In: *Journal of Modern Optics* 43.2 (Feb. 1996). DOI: 10.1080/09500349608232742.

[16] Jean-Francois Sauvage et al. “SAXO: the extreme adaptive optics system of SPHERE (I) system overview and global laboratory performance”. In: *Journal of Astronomical Telescopes, Instruments, and Systems* 2.2 (May 2016). DOI: 10.1117/1.JATIS.2.2.025003.

[17] Noah Schwartz et al. “Design of the HARMONI Pyramid WFS module”. In: *arXiv preprint arXiv:2003.07228* (2020).

[18] Roberto Tamai et al. “Status of the ESO’s ELT construction”. In: *Ground-based and Airborne Telescopes IX*. Vol. 12182. SPIE. 2022, pp. 437–453.

[19] Christophe Vérinaud. “On the nature of the measurements provided by a pyramid wave-front sensor”. In: *Optics Communications* 233.1-3 (2004), pp. 27–38.